Impact of Geological Heterogeneity on Early-Stage CO_2-Plume Migration: Sensitivity Study

Meisam Ashraf Knut-Andreas Lie Halvor M. Nilsen Arne Skorstad

November 29, 2011

1 Introduction

Underground sequestration of CO_2 produced from localized sources like power plants and oil and gas recovery sites has been proposed as a possible solution to reduce the rate of anthropogenic CO_2 emission into the atmosphere [5, 2]. Much of the technology required to inject CO_2 into saline aquifers, unminable coal seams, and abandoned reservoirs is already available from the petroleum and mining industry. However, before large-scale storage operations can be initiated, answers to practical questions regarding operational safety and the fate of the injected CO_2 need to be answered. The main concern for policy makers and the general public is the risk of leakage, i.e., how likely it is that the injected CO_2 (or highly saline brine) will migrate into water resources, active petroleum reservoirs, or back to the surface via conductive features like fractures and faults, through ill-plugged wells [10], or through caprocks broken by the high pressure imposed to the system during the injection operation. Likewise, there is a concern about pressure buildup, which may extend much further than the injected CO_2 plume (the effluent of CO_2 into brine). In other words, the operator of a potential injection site needs to maximize storage volumes while minimizing leakage risks and effects on areas surrounding the injection point.

The flow of CO_2 in the subsurface is governed by a very complex interaction between physical forces acting on the reservoir fluids and properties of the reservoir rock itself. To determine the fate of the injected CO_2, it is necessary to develop effective (numerical) models that can be used to accurately describe the pertinent flow dynamics during injection and the subsequent migration period. Moreover, the numerical models must also properly account for geological heterogeneity—i.e., variations in hydraulic conductivity and fluid storage—and how this heterogeneity influences the flow dynamics. Geological heterogeneity is recognized as a major control mechanism within petroleum production [3] and an important constraint on many aspects of quantitative hydrogeology. For this reason, much effort has been devoted to understand and represent geological heterogeneity in flow models, see e.g., [4]. The understanding of the geology of a specific reservoir or aquifer is typically limited and the description of the geological heterogeneity will usually have large uncertainties attached. If flow simulations are to be used to assess risks associated with a storage operation, the numerical flow model must properly account for the impact of uncertainty in the geological description. Yet, academic studies of CO_2 injection commonly employ simplified or conceptualized reservoir descriptions, in which the medium is considered (nearly) homogeneous, and instead focus on developing complex flow models, discretization schemes, and solvers.

Within oil recovery, the impact of geological uncertainty on production forecasts has been thoroughly investigated in the SAIGUP project [8, 6, 9], in which an ensemble of synthetic but realistic models of shallow-marine reservoirs were generated and several thousand cases were run for different production scenarios. The results showed that realistic variations in the structural and sedimentological description has a strong influence on production responses. Simulation of CO_2 storage involves temporal and spatial scales and density ratios that are quite different from those encountered in oil recovery. Potential storage sites may also have geological characteristics that differ from those seen in producible oil reservoirs. For these reasons, one cannot expect that knowledge of how geological heterogeneity impacts flow predictions of oil-water systems can be carried directly over to CO_2-brine systems relevant for CO_2 injection scenarios. Nevertheless, we will herein consider a scenario in which CO_2 is injected into an abandoned shallow-marine reservoir and use geological realizations generated as part of the SAIGUP project to study the impact of geological heterogeneity on the early-stage

migration of the CO_2 plume. How heterogeneity impacts the injection operation will be studied in a separate work, in which we also discuss more realistic pressure constraints on the injection operation.

Our work is a continuation of an early study reported in [1], which focused on a few primary flow responses. Herein, we will also include flow responses that relate more directly to leakage risk. In addition, we evaluate how curvatures in the relative-permeability model influences plume migration; this as a complement to previous studies of endpoint and hysteresis effects, see e.g., [11, 7].

2 Model Setup

In this study, we will consider a storage operation in which supercritical CO_2 is injected into a shallow-marine reservoir underneath a sealing caprock that forms a type of structural trap that is often seen in petroleum reservoirs. To represent the aquifer geology, we use an ensemble of synthetic models developed in the SAIGUP study [8]. In this study, data were collected from many different sources to develop representative, parametrized models that span realistic parameter intervals for progradational shallow-marine depositional systems with limited tidal influence [6]. An ensemble of geostatistical realizations were then made from the parametrized model, each having a heterogeneity and geometrical complexity as seen in real-life models of petroleum reservoirs. In our study, we have selected the following five parameters that altogether give 160 realizations:

Lobosity – is defined by the plan-view shape of the shoreline. As a varying parameter, lobosity indicates the level at which the shallow-marine system is dominated by each of the main depositional processes. Two depositional processes are considered in the SAIGUP study: fluvial and wave processes. The higher the amount of sediment supply provided from rivers is relative to the available accommodation space in the shallow sea, the more fluvial dominant the process will be. As the river enters the mouth of the sea, it can divide into different lobes and branches. Wave processes from the sea-side smear this effect and flatten the shoreline shape. Less wave effect produces more pronounced lobe shapes around the river mouths. Very high permeability and porosity can be found in the channeling branches, while dense rock with low permeability fills the space between them. Reservoir quality decreases with distance from the shore-face. We expect that the level of lobosity can have a considerable effect on the CO_2 injection and plume size in the aquifer. In this study, models of three levels of lobosity are used: flat shoreline, one lobe and two lobes, as illustrated in the upper row of Figure 1.

Barriers – Periodic floods result in a sheet of sandstone that dips, thins, and fines in a seaward direction. In the lower front, thin sheets of sandstone are interbedded with mud-stones deposited from suspension. These mud-draped surfaces will potentially act as significant barriers to both horizontal and vertical flow, and are modeled by transmissibility multipliers corresponding to three levels of coverage for the barrier sheet: low (10%), medium (50%), and high (90%), as illustrated in the middle row of Figure 1.

Aggradation – In shallow-marine systems, two main factors control the shape of the transition zone between river and basin: amount of deposition supplied by the river and the accommodation space that the sea provides for these depositional masses. One can imagine a constant situation in which the river is entering the sea and the flow slows down until stagnation. The deposition happens in a spectrum from larger grains depositing at the river mouth to fine deposits in the deep basin. If the river flux or sea level fluctuates, the equilibrium changes into a new bedding shape based on the balance of these factors. The SAIGUP data models cases in which, for instance, the river flux increases and shifts the whole depositional system into the sea. The angle at which the transitional deposits are stacked on each-other because of this shifting, is called aggradation angle. Three levels of aggradation are modeled here: low, medium, and high angles. The three parameter choices are illustrated in the bottom row of Figure 1, where we in particular notice how a low aggradation angle gives continuous facies layering parallel to the dip direction of the model.

Progradation – denotes the direction of the depositional dip. Two types are considered here: up and down the dominant structural dip. Because the model is tilted a little, this corresponds to the lobe direction from flank to crest or vice versa.

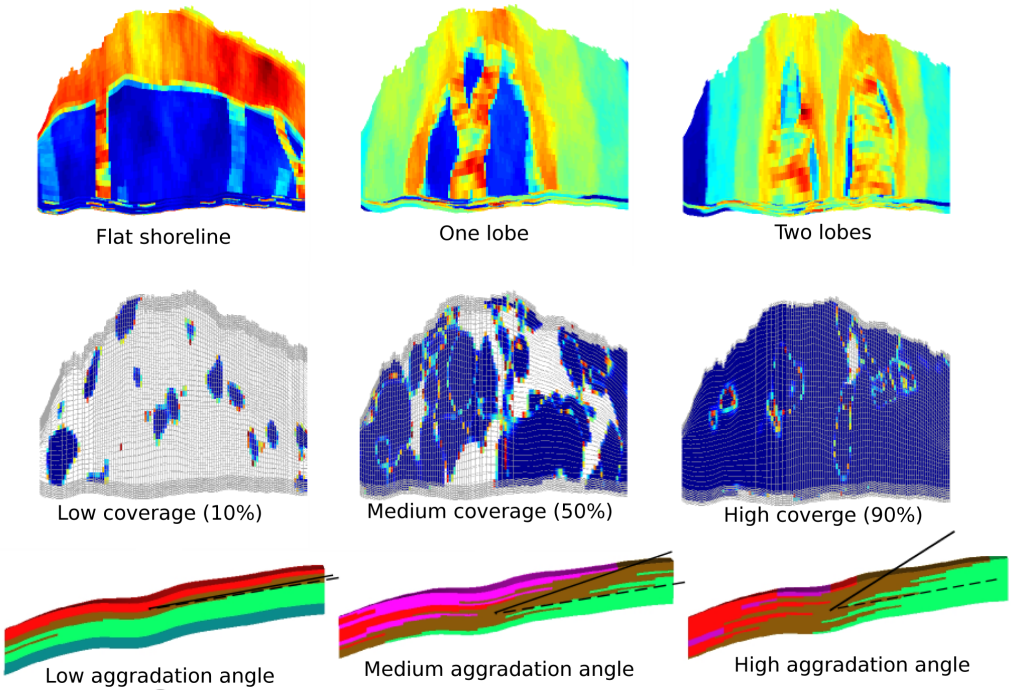

Figure 1: Illustration of geological parameters from the SAIGUP study: the top row shows three different lobosities for up-dip progradation (if the lobes flip over the long axis, we will have down-dip progradation); the middle row shows barriers representing different degrees of mud-draped coverage; and the bottom row shows aggradation angle.

Table 1: Geological features from the SAIGUP project included in this study. The last column reports markers used to distinguish different features in the plots.

Feature	Levels	Marker
Lobosity	flat, one-lobe, two-lobe	square, circle, diamond
Barrier	low(10%), medium(50%), high(90%)	small, medium, large
Aggradation	low(parallel layering), medium, high	blue, green, red
Progradation	up-dip, down-dip	first half, second half
Fault	unfaulted, open faults, closed faults	thin, medium, thick

Fault – are represented by three different parameters in the SAIGUP study: fault type, intensity, and transmissibility. Herein, we limit our study to compartment faults of medium intensity and consider three parameter choices: no faults, open faults, and closed faults.

Table 1 lists the markers (shape, size, color, thickness) that will be used to signify different parameters values in plots of simulation results later in the paper.

We will consider storage of forty million cubic meters of supercritical CO_2, which amounts to approximately 20% of the total pore volume in the aquifer and will be injected from a single well over a period of thirty years. After the injection period, seventy years of plume migration is simulated for all cases. If the medium was homogeneous, we would expect that the injection will create one big plume that moves upward because of the gravity force until it accumulates under the structural trap of the caprock, i.e., migrating from the injection point and upward to the crest of the aquifer. The idea is therefore to inject as deep as possible to increase the travel path and the volume swept by the plume before it reaches the crest. To this end, the injector is placed down in the flank and only completed in the three lowest layers of the aquifer. Hydrostatic boundary conditions are imposed on the sides, except at the faulted side on the crest, and no-flow boundary conditions are imposed on the top and bottom surfaces.

The injected CO_2 is assumed to be a supercritical fluid with density 700 kg/m^3 and viscosity 0.04 cP. The supercritical fluid is modeled as a dead oil with a formation factor of 1.1 at 0 bar and 0.95 at 400 bar. Brine is assumed to be slightly compressible ($3.03 \cdot 10^{-6}$ psi^{-1}) with density 1033 kg/m^3 and

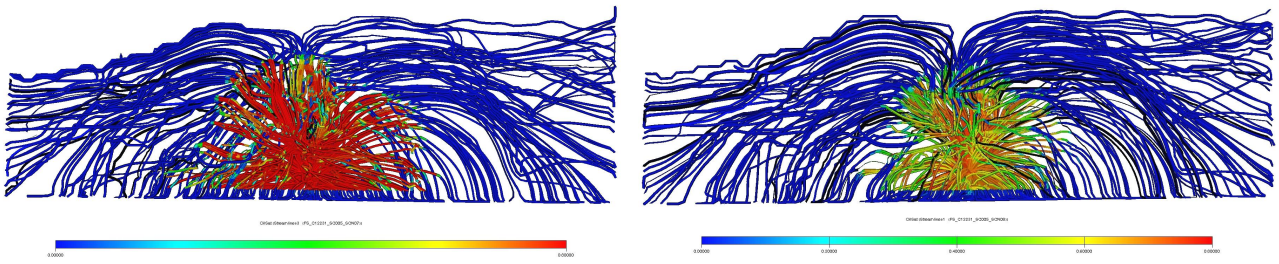

Figure 2: CO_2 saturation plotted on streamlines for linear relative permeabilities (left) and quadratic permeabilities (right).

viscosity 0.4 cP. The rock compressibility is set to $3 \cdot 10^{-7}$. For both fluids, we will use Corey-type relative permeability functions

$$k_{rCO_2} = (1 - S)^\alpha, \quad k_{rw} = S^\alpha, \qquad \alpha = 1, 2$$

where S denotes the saturation of brine normalized for end points 0.2 and 0.8.

3 Basic Flow Responses

In this section we will give a qualitative discussion of how some basic flow responses like the wave speeds of the plume migration, average aquifer pressure, mobile and residually trapped volumes, and plume sizes are affected by variations in the geological parameters.

3.1 Effect of relative permeability curvature

How the geological heterogeneity impacts the plume migration will depend upon the fluid model. We therefore start by discussing the choice of relative permeability functions. Previous studies have mainly looked at hysteresis and effects from saturation endpoints, see e.g., [7]. However, the curvature of relative permeability function will also play a significant role and in the following we will therefore consider both linear and quadratic relative permeability curves. In oil recovery processes, the efficiency of flooding increases by the higher viscosity of displacing fluid. For example in water-flooding, increasing the water viscosity using additives is a way to increase the process efficiency. For CO_2 storage, on the other hand, we are interested in mixing brine and CO_2 to increase the rate of dissolution; a lower viscosity of CO_2 compared to brine helps this aim.

With linear relative permeability and a CO_2 viscosity of tenth of the brine viscosity, there will be no sharp displacement front in the system and CO_2 invades the brine zone in a spectrum of rarefaction waves from zero to the maximum possible saturation (0.8 in our case). On the other hand, with quadratic relative permeability functions, there will be a sharp displacement front with a saturation around 0.4 followed by rarefactions.

To illustrate the different behavior of linear and quadratic relative permeabilities, we have picked one of the SAIGUP models which includes one shoreline lobe, medium level of barriers, high aggradation angle, up-dip progradation, and open faults. Figure 2 shows the CO_2 distribution resulting from the two different relative permeability functions. Although the streamline paths appear to be almost identical, there are significant differences in the extent of the plume and the saturation profile inside. With linear relative permeability and a CO_2 viscosity of tenth of the brine viscosity, there will be no sharp displacement front in the system and CO_2 invades the brine zone as a rarefaction fan from zero to the maximum possible saturation. In the left plot of Figure 2, this is observed as a spectrum of saturations ranging from zero to 0.8 and then a bank of constant saturation down to the injector (the red color region around the well). With quadratic relative permeabilities, on the other hand, there will be a sharp displacement front followed by a rarefaction fan. The front (with a saturation around 0.4) is recognizable followed by rarefactions down to the injector in the right plot of Figure 2.

In the simulation we observe that a significantly larger volume of injected CO_2 escapes through the down boundary in the quadratic case. The reason is that the mobility will be higher in the linear case and the wave speed at the tip of the rarefaction fan is significantly faster than the wave speed of the

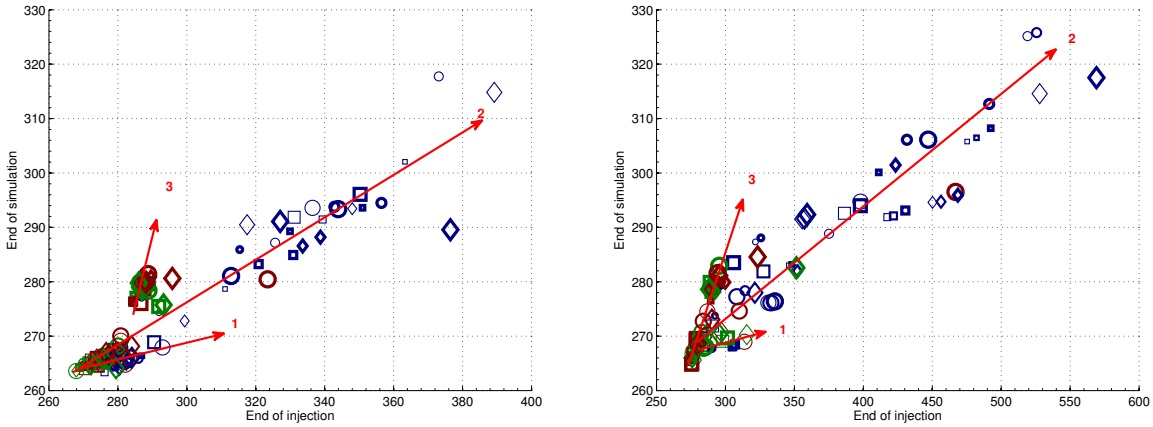

Figure 3: Cross-plot of average aquifer pressure at the end of simulation versus at the end of injection for linear (left) and quadratic (right) relative permeabilities.

displacement front for the quadratic case; compare the size of the two plumes in Figure 2. This means that the CO_2 plume will spread easier in the medium resulting in less flow through the boundary closest to the injector. Because of the lower mobility values in the quadratic case, more mass of CO_2 will be almost immobilized in the medium and the CO_2 plume will migrate very slowly compared with the linear case. Secondly, we observe higher pressures in the system during injection for quadratic permeabilities. The curvature of the quadratic curve gives lower mobility of CO_2 for small saturation values, and thence higher injection pressure is required to move the flow in the medium.

3.2 Pressure responses

The average aquifer pressure in general shows a sharp jump at the start of injection and a declining trend during injection and plume migration caused by pressure release through the open boundaries. (Specifying different boundary conditions would have resulted in different pressure trends). Figure 3 shows cross-plots of the average aquifer pressure at the end of injection and end of simulation for our two different choices of relative permeability functions. In both plots, one can recognize three different trends which have been indicated by three straight lines. The first trend, which has the lowest slope, represents cases with large pressure variation during injection and small range of pressure variation during the migration phase that follows after the end of injection. In these cases, the heterogeneity of the medium forms channels towards the open boundaries through which the injection pressure is released, resulting in low aquifer pressure at the end of simulation. The second trend, represents cases in which the heterogeneity affects injection, gravity segregation, and flow through open boundaries. In particular, we observe that most cases that have high injection pressure correspond to a low aggradation angle, for which low vertical permeability forces the injected CO_2 plume to move relatively slow in the lowest, poor-quality layers before migrating up towards the caprock. This increases the pressure in the domain during injection and keeps a higher pressure gradient to the open boundaries. In the third trend, the heterogeneity makes chambers and compartments in which the pressure increases during injection and then remains high. Cases with closed faults are of this class. The heterogeneity in these cases affects the gravity segregation process more than in the two other trends because of faults and a high level of barriers.

We also see the effect of curvature in the relative permeabilities by comparing the two plots. Higher range of pressure variations is observed during injection for the nonlinear relative permeability runs. Moreover, nonlinear relative permeability gives lower mobility which leads to higher pressure build-up during injection. This means that longer time is required for the pressure to be released through the open boundaries after injection and more cases therefore follow the second and third trend.

More details about the bottom-hole pressure will be given in a forthcoming paper, in which we also will discuss more realistic constraints on the injection operation.

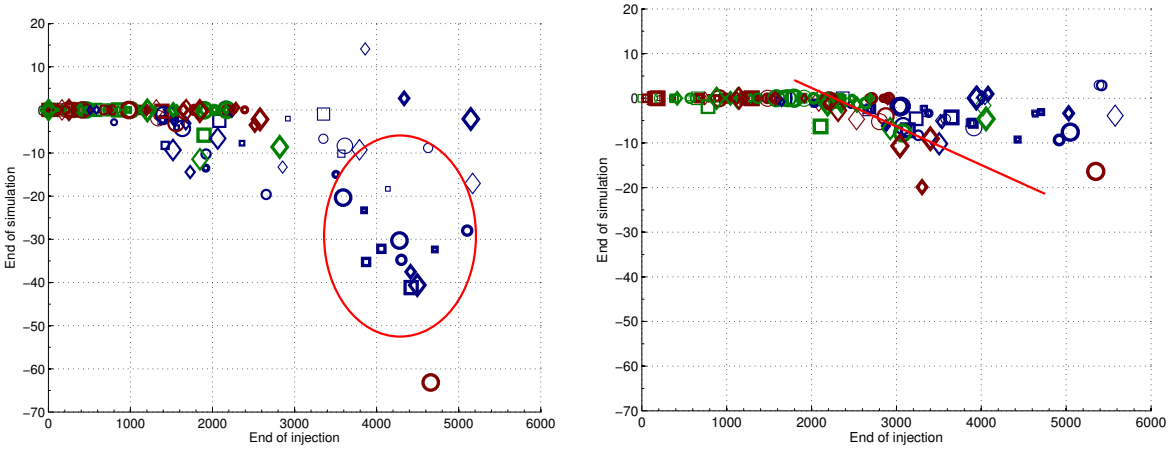

Figure 4: Cross-plot of CO_2 flux out over the down-dip boundary for linear (left) and quadratic (right) relative permeabilities. Positive values represent outward fluxes and negative values represent inward fluxes.

3.3 Plume migration

The direction in which the CO_2 plume moves in the medium will primarily impact the amount of residual (and structural) trapping, but as we will see later, also significantly change the risk for leakage through breaches and holes in the caprock. When evaluating the safety of a long-term storage operation, there are several potentially conflicting aspects that need to be considered with regard to plume migration. On one hand, we prefer the plume to spread out laterally to enhance residual trapping and mixing of CO_2 and brine, while on the other hand we want to confine the plume to the smallest volume possible to minimize the the risk of leakage and contamination into other aquifers, minimize the contact with potential leakage points and simplify monitoring operations. To investigate this aspect, we will study the sweep efficiency in local regions. On the other hand, if a big movable plume connects with a leakage pathway through the caprock, large volumes of CO_2 may escape, and for this reason, it may be better if the injected CO_2 splits into many small plumes. In our analysis, we will therefore also consider the number of plumes and their volumes.

3.3.1 Boundary fluxes

The sweep efficiency of the CO_2 plume, i.e., the percentage of the aquifer volume that has been in contact with CO_2, is positively correlated with the amount of residual trapping (and mixing of CO_2 and brine). Herein, we will consider the flux out of the open boundaries as an indirect measure of volumetric sweep efficiency. The model has open boundaries on three sides, which are modeled by imposing huge pore-volumes multipliers in the outer cells, while no-flow boundary conditions are imposed along the top faulted side. Using large pore-volume multipliers to represent an open boundary enables us to model flow both in and out of the domain, and this way, we can represent volumes of CO_2 leaving and later re-entering the aquifer. (In addition, this method will contribute to eliminate effects from Dirichlet type boundary conditions).

The lower boundary is closest to the injection point and hence the most likely place that injected CO_2 volumes will be lost. Figure 4 shows two cross-plots of the CO_2 across this boundary at the end of injection and the end of simulation. Towards the end of injection, most cases have positive flux values, which means that parts of the main plume connected to the injection point has been forced to leave the domain in the down-dip direction by the increased injection pressure. However, after injection stops, many cases have small negative fluxes, which means that a small volume of CO_2 reenters the domain. Once again, we observe that cases with low aggradation angle stand out from the rest. In these cases, the injected plume is almost entirely confined to the bottom of the model because of poor vertical communication. Hence, a large portion of the injected volume will be forced out of the domain in the down-dip direction. After the end of injection, gravity forces will gradually cause some of these lost volumes to move up-dip again and reenter the domain. We notice that cases with closed faults (shown in the red circle in the left plot of Figure 4) show a relatively higher return

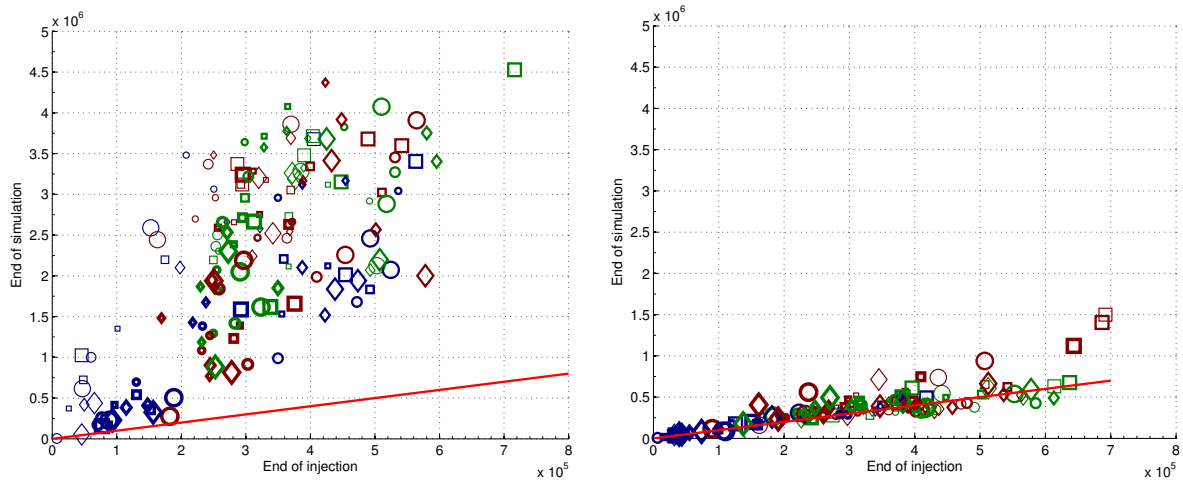

Figure 5: Residually trapped volumes for linear (left) and quadratic (right) relative permeabilities. Cases on the red lines have the same values at the end of injection and end of simulation.

flux for the linear relative permeability function. With nonlinear relative permeability function, some of the cases follow a linear trend (shown by the red line in the right-hand plot), in which the return flux is proportional to the outward flux.

3.3.2 Total mobile/residual CO_2

Residual trapping occurs when the CO_2 saturation is below the residual saturation value of 0.2. Although the residually trapped CO_2 is free to move in a molecular sense on the microscale, the corresponding bulk volume is considered immobile on the macro scale. To reduce the risk of leakage, it is therefore important to obtain an efficient volumetric sweep that will maximize the residual volumes and minimize the mobile volumes. Herein, we will define residually trapped volumes as volumes in which the CO_2 saturation is below the residual value of 0.2. Notice that with this definition, all mobile volumes (in which the saturation exceeds 0.2) will contain a residual portion of CO_2 that is not free to escape. This portion will eventually become residually trapped if the saturation of the mobile CO_2 decreases to the residual value.

Figure 5 shows cross-plots of the total residual volume at the end of injection and end of simulation. Drainage is the dominant flow process during injection. When injection ceases, the plume migration turns into a imbibition-dominated process which increases the residual trapping of CO_2. With linear relative permeability, the imbibition process takes place relatively fast, and the residual volume increases significantly from end of injection to end of simulation. Once again, low-aggradation cases form notable exception having small amounts of residual trapping. The reason is primarily that significant volumes have been lost over the down-dip boundary, and secondarily that the (vertical) sweep is limited because the CO_2 plume is confined to the lower layers of the reservoir during most of the simulation time.

With quadratic relative permeabilities, the migration process is significantly slower and many cases have almost the same residual volume at the end of injection and end of simulation. As already discussed, the curvature of the relative permeability function does not have a considerable influence on the flow paths (compare the streamline paths in Figure 2). Compared with the results in the left right plot of Figure 5, we therefore ultimately expect a significant increase in residual trapping before the plume settles; this prognostication has been confirmed for a few (arbitrary selected) cases by computing the plume migration for more than ten thousand years. We also observe that in some cases the residual volumes *decrease* after injection ceases. This is caused by mobile CO_2 invading zones of residual CO_2, thereby turning residual volumes into mobile volumes according to the definition of residual trapping used herein. These cases are therefore likely to be influenced by hysteresis effects, which for simplicity have been disregarded in this study.

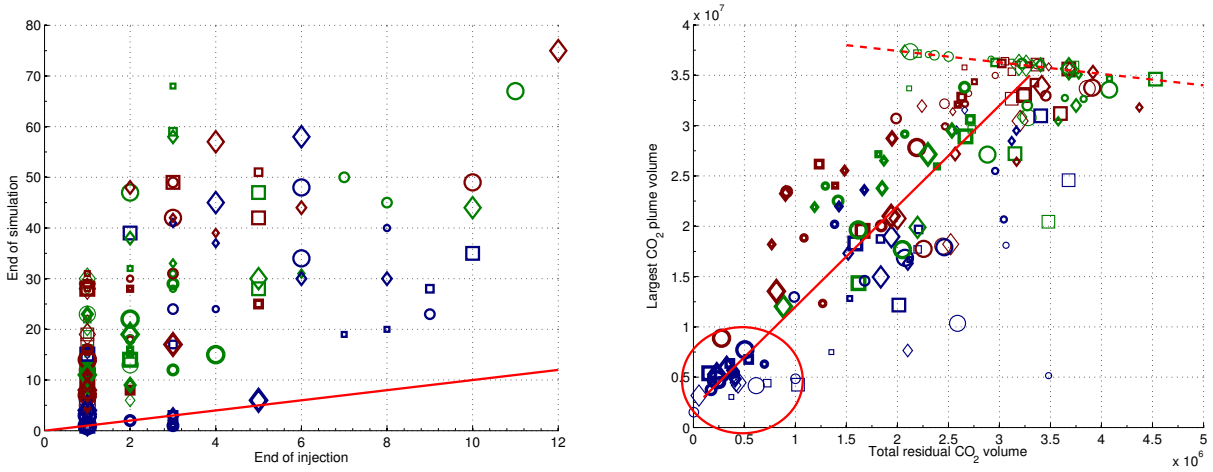

Figure 6: The cross-plot to the left shows the number of CO_2 plumes at the end of simulation versus the number of plumes at the end of injection for linear relative permeability function. The right plot shows the volume of the largest CO_2 plume versus the volume of residual CO_2 at the end of simulation.

3.3.3 Connected CO_2 volumes

In the next section, we will study the risk of leakage through the caprock. To this end, we will assume that all mobile CO_2 connected to a leakage point will escape through that point. Hence, it is preferable if the total mobile CO_2 volume is split into smaller plumes rather than forming a big mobile plume. Moreover, the surface area per volume increases by splitting the plume (assuming constant plume shape) and this helps residual trapping (and mixing of brine and CO_2).

During injection, the flow support from the well builds a connected mass of CO_2 shaping one or a few big plumes. When the injection ceases, the CO_2 starts distributing in the medium and plumes may split because of branches in the flow paths created by heterogeneity. The plot to the left in Figure 6 shows how the number of plumes increases significantly in most cases during the migration phase, except for a few low-aggradation cases for which the injected plumes stay intact or reform into a single plume.

The right plot in Figure 6 shows the volume of the largest CO_2 plume versus the residual trapping. Here, we see two major trends indicated by a solid and a dashed line. The solid line, having a positive slope, represents cases that loose CO_2 through the open boundaries, mainly through the one closest to the injection point. As a consequence, less CO_2 volume exists in the system and the size of the largest plume will be smaller. Hence, less volume will be swept while the plume migrates upward (if it does), which again means that less CO_2 is residually trapped. In particular, we notice the cases inside the ellipse which are the same cases that had large CO_2 volumes escaping through the down-dip boundary as shown in Figure 4. The dashed line with negative slope corresponds to cases for which almost all of the injected CO_2 stays inside the domain. These cases show a small range of variation for the largest plume size and are reflecting the effect of different heterogeneity features on the residual trapping process. Because equal volumes of CO_2 are injected in all cases, we notice that the bigger the largest plume is, the smaller the residual volume will be.

4 Analysis of Parameter Impact

The main purpose of the current study is to investigate how geological heterogeneity impacts the formation of a CO_2 plume during injection and during the early-stage migration after injection ceases. In this section, we will therefore perform a simple 'sensitivity analysis' that will tell us something of how the different geological parameters impact the flow responses discussed in the previous section. The five geological parameters impact the flow responses to different degrees; some parameters are more influential during injection, others take effect when the migration starts after injection has ceased, and some are influential both during injection and migration. Comparing the relative impact of the different parameters will indicate which of the parameters are most important to represent accurately when modeling a specific aquifer of the type considered herein.

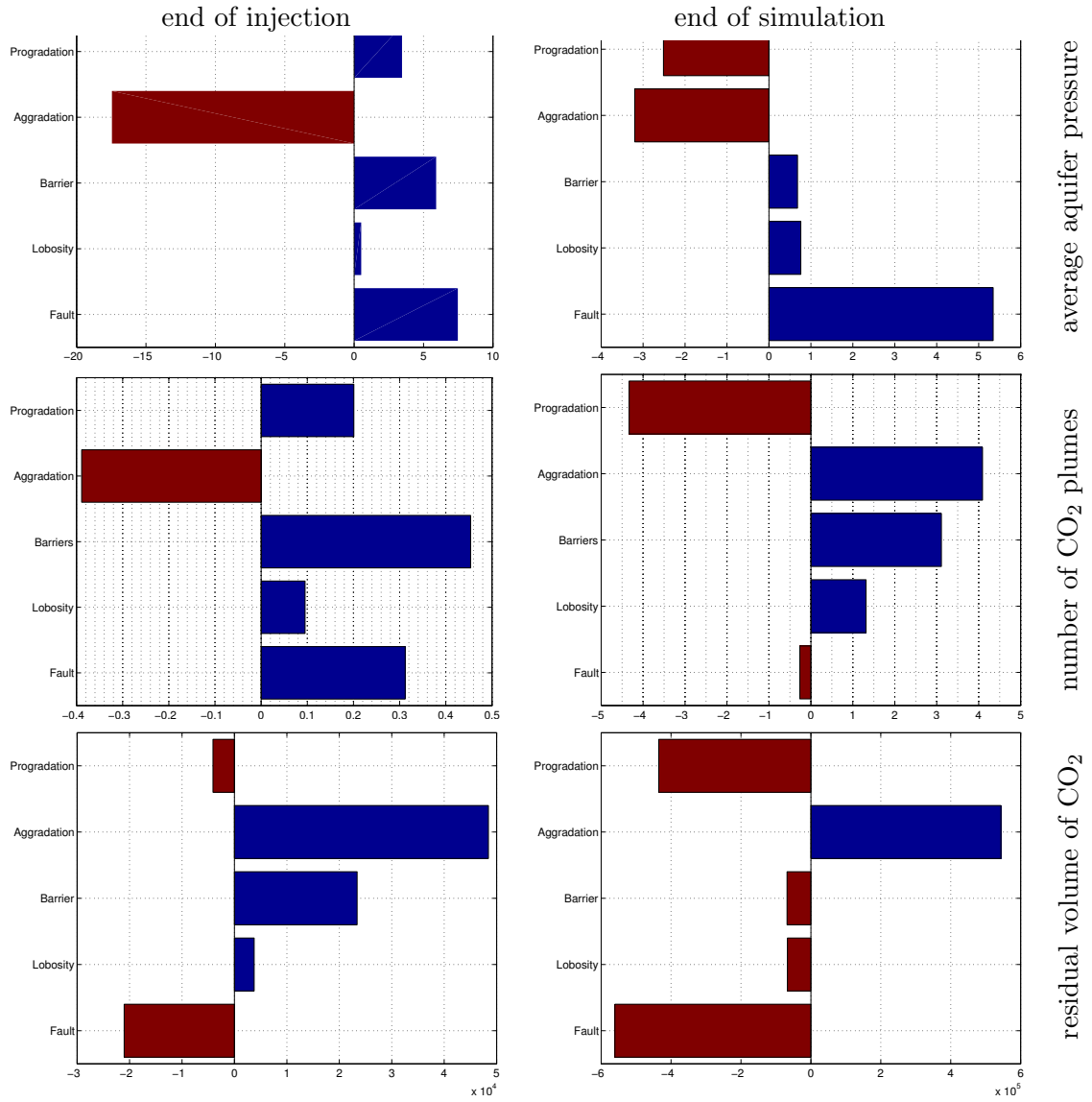

Figure 7: Sensitivities to different geological features at end of injection and end of simulation for the average aquifer pressure, number of CO_2 plumes, and residual volume of CO_2.

To quantify the relative impact of each geological parameter, we will define a normalized gradient for each feature. We will use barriers as an example to explain the analysis. There are three levels of barriers: low, medium and high. Suppose that we want to calculate the sensitivity of the number of plumes with respect to the level of coverage for the barrier sheets. We do this in two steps: first we average the number of plumes for cases of the same level of barriers. Having three levels of barrier, this results in three averaged plume numbers corresponding to each level of barriers. In the next step, we fit a line through these three points and calculate the inclination of this line which represents how the number of plumes increases if the barrier parameter increases one level. For other features like fault and lobosity, we follow the same procedure. We use three levels for each feature and fit a trend through these three points. For example, the first level of fault criteria relates to unfaulted cases, the second relates to open faults, and the third represents cases with closed faults.

Figure 7 shows the sensitivity for three different flow responses. In the upper row, we see that during injection the average aquifer pressure is most influenced by aggradation, while at the end of simulation the most influential feature is the fault specification. The lack of good vertical communication for low aggradation angles means that the CO_2 is confined to the lower (poor quality) layers and relatively high pressures must be imposed to inject the required amount of CO_2 into the aquifer. For higher angles, the CO_2 can flow more easily upward through channels with higher permeabilities and less pressure support is required. Hence, the negative gradient. After the injection ceases, the dominating force is gravity, the main flow direction is vertical, and the pressure is now mostly affected by faults. If the faults are closed, they will prevent the release of pressure through the open

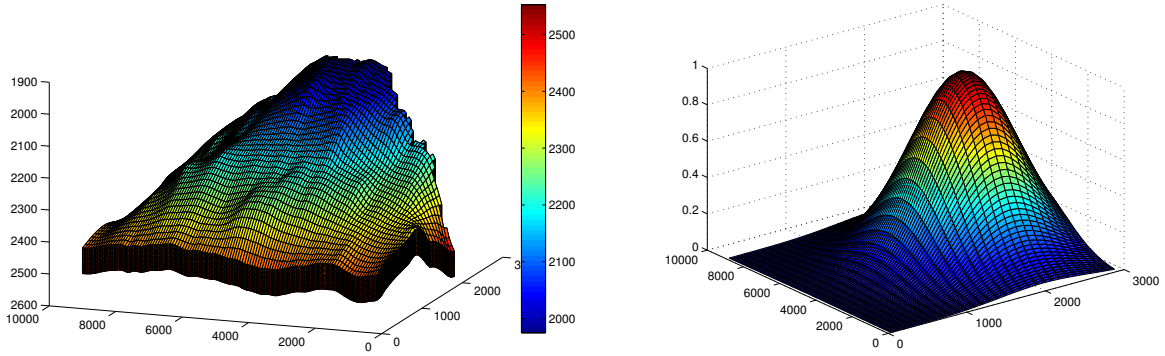

Figure 8: The left plot shows a sample grid geometry with depth values shown in meters. The right plot shows the Gaussian probability distribution for point leakage through the caprock. The distribution is centered at a point on the crest which is in the same slice as the injection point.

boundaries. We also observe that the effect of progradation switches from positive to negative after the injection is stopped: Injecting in the up-dip direction is easier than injecting down-dip, while a down-dip deposition opens up more conductive medium in front of the plume as it migrates towards the crest.

The second row in Figure 7 shows the sensitivity in the number of CO_2 plumes. During injection, the barriers coverage is the most influential parameter, because mud-draped surfaces enhance the lateral flow and force the plume to split rather than migrating towards and accumulating at the crest. Aggradation has a similar effect: the lower the angle is, the more the injected CO_2 spreads out laterally. At the end of simulation, progradation and aggradation are the dominant effects. In particular, higher aggradation angle improves the segregation across layers and thus increases the splitting of plumes through heterogeneities. The impact of the faults is more significant than the figure shows: open faults contribute to split plumes, while the unfaulted cases and the cases with closed faults introduce a small number of plumes. In average, the positive and negative contributions cancel out to almost zero. Finally, the bottom row in Figure 7 reports sensitivities for the total residual volume. Here, aggradation is the most influential parameter during injection and faults the most important parameter during the migration phase.

Similar analyzes have been conducted for other flow responses as well. Altogether, our sensitivity study shows that aggradation is the parameter that has most impact on the flow responses we have studied. Aggradation has either the largest or the second largest gradient during both injection and migration for almost all responses. The faulting has the second highest impact. Mostly effected by closed fault, the fault parameter influences the storage capacity and the extent to which a CO_2 plume accumulates under the caprock. Barriers play a dominating role for the splitting of plumes during injection, whereas the progradation affects the gravity segregation through conductive channels during the migration phase and the volume available to flow in the dip direction. Finally, lobosity has small impact compared to the other parameters and can therefore likely be ignored for the fluid responses considered above. However, lobosity has a considerable effect on the lateral movement and splitting of plumes during the migration period and may therefore have a more significant impact on the estimates of point leakage.

5 Leakage Risk

The SAIGUP study does not supply any information about the caprock and its geomechanical properties. We are therefore only able to conduct a conceptual study of the risk associated with point leakage through imperfections in the caprock. To this end, we assume that each point on the top surface has a prescribed probability for being a leakage point. As a simple example, we will assume that the probability for point leakage follows a standard 2D Gaussian distribution centered at a given point on the crest, see Figure 8. Moreover, we will assume that all mobile CO_2 (except for the residual portion) will escape through the caprock if a plume comes in contact with a leakage point. We have seen above that the heterogeneity and tilt of the medium will cause the injected CO_2 to be distributed

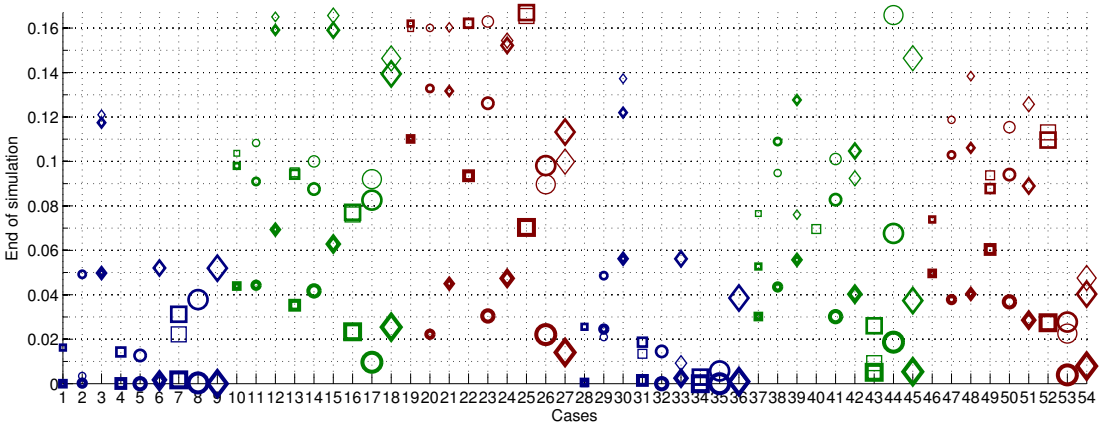

Figure 9: Leakage risk at end of simulation for linear relative permeabilities.

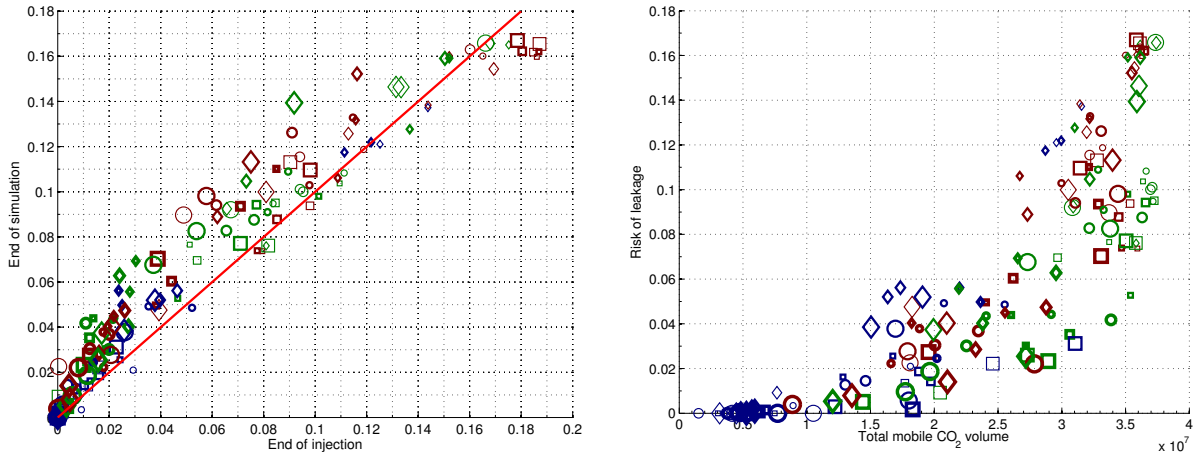

Figure 10: The left plot shows a cross-plot of leakage risk for linear relative permeability function. The right plot shows mobile CO_2 volume versus leakage risk at the end of simulation.

under the caprock as a number of plumes with variable sizes. For each cell along the top surface, we now define the risk as the probability of point leakage weighted by the size of the CO_2 plume that the cell is part of. We then sum the values for all the topmost cells, normalize this sum, and use the resulting single number as a measure of leakage risk. The worst possible case would be if all the injected CO_2 volume forms a mobile plume that contacts every point along the top surface; this gives a risk value equal to one. For all actual cases, however, the risk value will be less than one because not all of the CO_2 will be mobile (because of residual trapping and loss of volumes across the open boundaries), because the mobile volume may form more than one plume, or because not all the mobile volume has reached the top due to reduced vertical mobility.

Figure 9 shows the resulting leakage risks for all cases at the end of simulation computed using linear relative permeabilities. Similarly, the left plot in Figure 10 shows how the risk develops during the seventy year period from the end of injection to the end of simulation, whereas the right plot shows a cross-plot of the leakage risk versus the total volume of mobile CO_2. The plots lead to the rather obvious conclusion that improved vertical connection will increase the risk of leakage through possible imperfections in the caprock and that there is a positive correlation between the volume of mobile CO_2 in the system and leakage risk. However, we also observe that there are cases which have zero leakage risk. These are cases with low aggradation, for which the flow stays in the injected layers and moves laterally towards the open boundaries, resulting in a low amount of mobile CO_2 in the system. Furthermore, these cases have (almost) no cross-layered CO_2 movement, which means that (almost) no CO_2 reaches the top surface. In other words, the low-aggradation cases, which have seemed to be infeasible because of high injection pressure, larger lateral spread, and loss of volumes through the open boundaries in our discussion in the previous two sections, here appear as the most feasible with

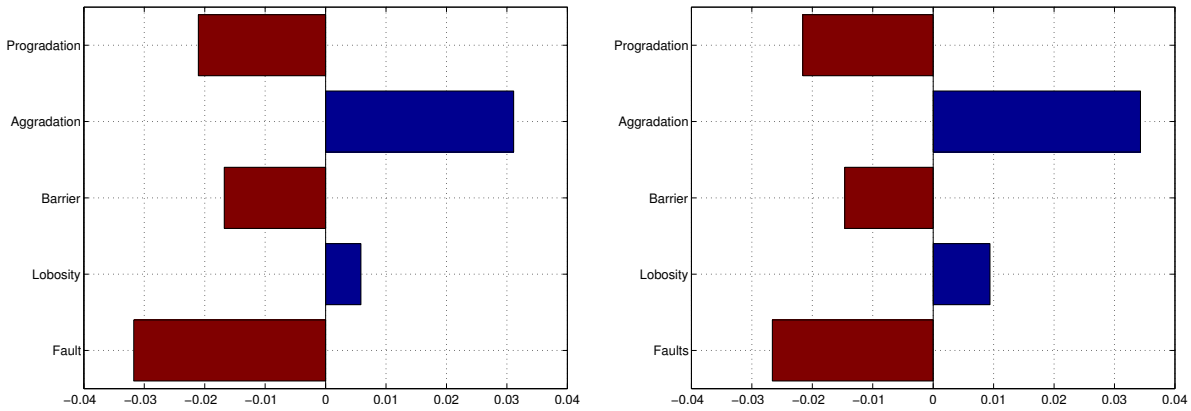

Figure 11: Sensitivity of the leakage risk with respect to the five geological parameters at the end of injection (left) and end of simulation (right).

respect to the chosen risk measure.

Figure 11 shows gradients for the leakage risk. Although less pronounced during injection time, the gravity force makes a major plume body attached to the crest both during the injection time and afterwards. Hence, we see that the leakage-risk sensitivity shows almost the same profile at end of injection and end of simulation. This can also be observed in Figure 10. The sensitivity is slightly less during injection compared to end of simulation, because more CO_2 will be below the caprock at end of simulation. This overtakes the effect of mobile volume reduction due to residual trapping process and the increase in the number of plumes at end of simulation, which both result in less risk of leakage.

Once again, aggradation angle and fault criteria are the two most influential features. Increasing the aggradation angle improves the vertical communication and contributes to increase the formation of CO_2 plumes below the caprock. Closed faults limit the movement of the plume and result in less accumulation below the caprock, whereas open faults generally increase the upward migration of plumes.

6 Conclusions

Herein, we have presented a study of how various geological parameters influence the injection and early-stage migration of CO_2 in progradational shallow-marine systems. One hundred and sixty equally probable realizations have been considered and several flow responses related to storage capacity and risk of point leakage have been calculated at the end of injection and after seventy years of gravity-dominated plume migration.

First of all, we have investigated the effect of relative permeability curvature by comparing the results of linear and quadratic relative permeability curves. The results show that linear relative permeabilities give significantly higher wave speeds that lead to earlier accumulation of CO_2 under the caprock, and will for this reason give conservative estimates of the plume migration and the risk associated with point leakage after a prescribed number of years.

Second, and more important, we have demonstrated and discussed how the heterogeneity induced by different geological parameters give large variations in flow responses. Each geological feature will influence the flow behavior and can result in local/global pressure build-up or pressure drop, enhance the flow direction, hinder the flow in the medium, or lead to loss of injected volumes over the open boundaries, and may induce different effects during the injection and plume migration. Specifically, we have demonstrated how variation in aggradation angle, fault criteria, and progradation direction significantly change the flow direction within the medium and hence impact the residual trapping and formation of movable CO_2 plumes under the caprock. Barriers are important during injection and must be modeled more carefully if the study focuses on injection operations.

Altogether, our study shows that geological heterogeneity has a major impact on the injection and formation of a CO_2 plume and the subsequent early-stage migration of this plume. A predictive study should therefore incorporate realistic estimates of geological uncertainty to provide reliable forecasts of operational risks and the long-term fate of injected CO_2.

References

[1] M. Ashraf, K.-A. Lie, H. M. Nilsen, J. M. Nordbotten, and A. Skorstad. Impact of geological heterogeneity on early-stage CO_2 plume migration. In J. Carrera, editor, *Proceedings of the XVIII International Conference on Water Resources (CMWR 2010)*, Barcelona, Spain, 2010. CIMNE.

[2] P. J. Cook, A. Rigg, and J. Bradshaw. Putting it back where it came from: Is geological disposal of carbon dioxide an option for australia. *Australian Petroleum Production and Exploration Association Journal*, 1, 2000.

[3] S. P. Dutton, W. A. Flanders, and M. D. Barton. Reservoir characterization of a permian deep-water sandstone, East Ford field, Delaware basin, Texas. *AAPG Bulletin*, 87(4):609, 2003.

[4] T. T. Eaton. On the importance of geological heterogeneity for flow simulation. *Sedimentary Geology*, 184(3-4):187–201, 2006.

[5] B. Hitchon. *Aquifer disposal of carbon dioxide: hydrodynamic and mineral trapping: proof of concept*. Geoscience Pub., 1996.

[6] J. A. Howell, A. Skorstad, A. MacDonald, A. Fordham, S. Flint, B. Fjellvoll, and T. Manzocchi. Sedimentological parameterization of shallow-marine reservoirs. *Petroleum Geoscience*, 14(1):17–34, 2008.

[7] R. Juanes, E. J. Spiteri, F. M. Orr Jr, and M. J. Blunt. Impact of relative permeability hysteresis on geological CO_2 storage. *Water Resources Research*, 42:W12418, 2006.

[8] T. Manzocchi, J. N. Carter, A. Skorstad, B. Fjellvoll, K. Stephen, J. A. Howell, J. D. Matthews, J. J. Walsh, M. Nepveu, C. Bos, J. Cole, P. Egberts, S. Flint, C. Hern, L. Holden, H. Hovland, H. Jackson, O. Kolbjørnsen, A. MacDonald, P. A. R. Nell, K. Onyeagoro, J. Strand, A. R. Syversveen, A. Tchistiakov, C. Yang, G. Yielding, and R. W. Zimmerman. Sensitivity of the impact of geological uncertainty on production from faulted and unfaulted shallow-marine oil reservoirs: objectives and methods. *Petroleum Geoscience*, 14(1):3–15, 2008.

[9] J. D. Matthews, J. N. Carter, K. D. Stephen, R. W. Zimmerman, A. Skorstad, T. Manzocchi, and J. A. Howell. Assessing the effect of geological uncertainty on recovery estimates in shallow-marine reservoirs: the application of reservoir engineering to the saigup project. *Petroleum Geoscience*, 14(1):35–44, 2008.

[10] J. M. Nordbotten, D. Kavetski, M. A. Celia, and S. Bachu. A semi-analytical model estimating leakage associated with CO_2 storage in large-scale multi-layered geological systems with multiple leaky wells. *Under Review at: Environmental Science and Technology*, 2008.

[11] E. Spiteri, R. Juanes, M. Blunt, and F. Orr. Relative-permeability hysteresis: Trapping models and application to geological CO_2 sequestration. In *SPE Annual Technical Conference and Exhibition*, 2005.